THE JOURNAL OF PHYSICAL CHEMISTRY A
A JOURNAL OF THE AMERICAN CHEMICAL SOCIETY

pubs.acs.org/JPCA

Article

Rotational Spectroscopy of 1-Cyano-2-methylenecyclopropane (C_5H_5N)—A Newly Synthesized Pyridine Isomer

Dairen R. Jean, Samuel A. Wood, Brian J. Esselman, R. Claude Woods,* and Robert J. McMahon*

Cite This: *J. Phys. Chem. A* 2024, 128, 1427−1437

Read Online

ACCESS | Metrics & More | Article Recommendations | Supporting Information

ABSTRACT: The gas-phase rotational spectrum of 1-cyano-2-methylenecyclopropane (C_1, C_5H_5N), an isomer of pyridine, is presented for the first time, covering the range from 235 to 500 GHz. Over 3600 *a*-, *b*-, and *c*-type transitions for the ground vibrational state have been assigned, measured, and least-squares fit to partial-octic A- and S-reduced distorted-rotor Hamiltonians with low statistical uncertainty (σ_{fit} = 42 kHz). Transitions for the two lowest-energy fundamental states (ν_{27} and ν_{26}) and the lowest-energy overtone ($2\nu_{27}$) have been similarly measured, assigned, and least-squares fit to single-state Hamiltonians. Computed vibration−rotation interaction constants (B_0-B_v) using the B3LYP and MP2 levels of theory are compared with the corresponding experimental values. Based upon our preliminary analysis, the next few vibrationally excited states form one or more complex polyads of interacting states *via* Coriolis and anharmonic coupling. The spectroscopic constants and transition frequencies presented here form the foundation for both future laboratory spectroscopy and astronomical searches for 1-cyano-2-methylenecyclopropane.

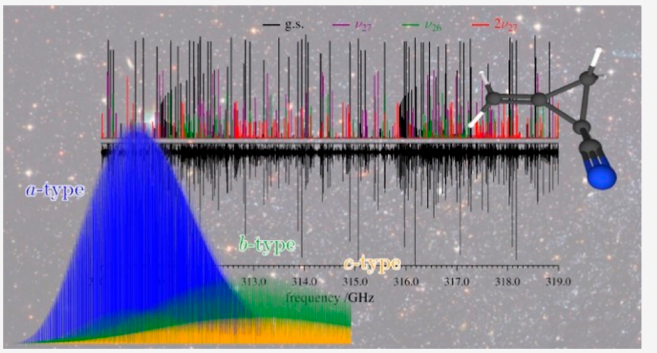

INTRODUCTION

Approximately 300 molecules have been detected in the interstellar medium (ISM) and more than 25% are nitriles. The unusually high proportion of nitriles is due, in part, to their typically large dipole moments, which result in sufficiently intense rotational transitions to be detectable by radio-astronomy.[1,2] We have a strong interest in studying organic nitriles, particularly the nitrile-containing isomers of pyridine[3−8] and aryl nitriles/isonitriles.[9−14] Our work on aryl nitriles and isonitriles has primarily focused on characterizing their rotational spectra to provide the necessary data to enable their use as potential tracer molecules for the corresponding parent species, *e.g.*, furan, benzene, pyridine, pyridazine, pyrimidine, and pyrazine. For instance, neither benzene nor pyrazine possesses a permanent dipole moment, and as a result, neither can be detected by radioastronomy. Furan, pyridine, pyridazine, and pyrimidine possess permanent dipole moments. Nevertheless, neither they nor any other hetero-aromatic compounds have been successfully detected in the interstellar medium.[15−23] Similarly, isomers of pyridine (**1**−**6**, Figure 1) could serve as tracer molecules for pyridine. A recent detection of (*E*)-1-cyano-1,3-butadiene (***E*-1**), an isomer of pyridine, in the GOTHAM observations of TMC-1 especially motivates further study of pyridine isomers.[24]

1-Cyano-2-methylenecyclopropane (**7**, C_1, C_5H_5N, Figure 2), a highly prolate, asymmetric top (κ = −0.85), is a newly synthesized structural isomer of pyridine. It possesses strong dipole components along all three principal axes (μ_a = 3.7 D,

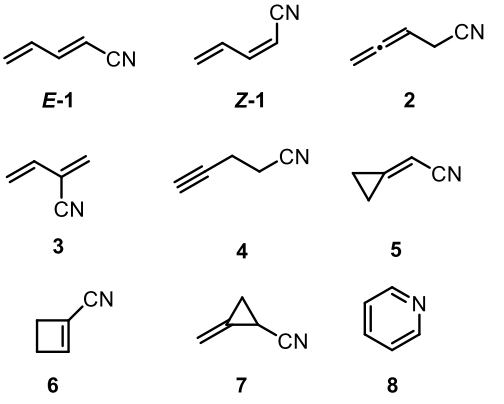

Figure 1. C_5H_5N isomers that have been studied by rotational spectroscopy: (*E*)-1-cyano-1,3-butadiene (***E*-1**),[6,25] (*Z*)-1-cyano-1,3-butadiene (***Z*-1**),[6,25] 4-cyano-1,2-butadiene (**2**),[6,25] 2-cyano-1,3-butadiene (**3**),[7] 4-cyano-1-butyne (**4**),[3] (cyanomethylene)cyclopropane (**5**),[5] 1-cyanocyclobutene (**6**),[8] 1-cyano-2-methylenecyclopropane (**7**), and pyridine (**8**).[26]

Received: December 6, 2023
Revised: January 14, 2024
Accepted: January 17, 2024
Published: February 14, 2024

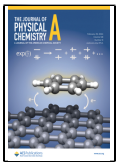

Downloaded via UNIV OF WISCONSIN-MADISON on March 8, 2024 at 21:22:01 (UTC).
See https://pubs.acs.org/sharingguidelines for options on how to legitimately share published articles.

ACS Publications
© 2024 American Chemical Society

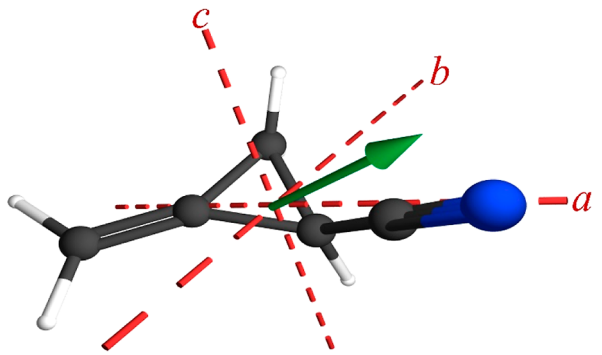

Figure 2. 1-Cyano-2-methylenecyclopropane (7, C_1, C_5H_5N) structure with principal inertial axes and dipole moment (green arrow; μ_a = 3.7 D, μ_b = 1.5 D, and μ_c = 0.94 D, MP2/cc-pVTZ).

μ_b = 1.5 D, and μ_c = 0.94 D, MP2/cc-pVTZ), making it an appealing molecule for laboratory study and for a radio-astronomical search. 1-Cyano-2-methylenecyclopropane (7) is higher in energy than pyridine (52 kcal/mol, MP2/cc-pVTZ) due, in part, to its strained three-membered ring and lack of aromaticity. Intriguingly, seven molecules with three-membered rings have been found in the interstellar medium to date: cyclopropenylidene (c-C_3H_2),[27] cyclopropynyl radical (c-C_3H),[28,29] ethynyl cyclopropenylidene (c-C_3HCCH),[30] cyclopropenone (c-H_2C_3O),[31] ethylene oxide [c-$CH_2(O)CH_2$],[32,33] propylene oxide [$CH_3CH(O)CH_2$],[34] and the bicyclic cluster SiC_3.[35] Herein, presented for the first time is a detailed analysis of the rotational spectra of the ground vibrational state, the first two fundamental states, and the lowest-energy overtone state of 1-cyano-2-methylenecyclopropane (7), covering the frequency range from 235 to 500 GHz. Interstellar detection of molecules *via* radioastronomy requires either specific transition frequencies that have been experimentally measured in the laboratory or a set of experimentally determined spectroscopic constants that can predict transitions with sufficiently high accuracy and precision. The transitions and spectroscopic constants presented in this work should serve as a basis for the search for this molecule in an interstellar medium over a wide frequency range.

EXPERIMENTAL AND COMPUTATIONAL METHODS

Synthesis. 1-Cyano-2-methylenecyclopropane (7) was prepared as shown in Scheme 1. A rhodium acetate-catalyzed cyclopropanation reaction of ethyl diazoacetate afforded the cyclopropane ring in **9**, followed by the elimination of HBr to generate the π bond in **10**. The ester **10** was converted to the corresponding amide **11**, which was subsequently dehydrated by treatment with phosphoric anhydride to afford 1-cyano-2-methylenecyclopropane (7). The synthetic details and spectroscopic characterization of synthetic intermediates are available in our contemporaneous work on the photoisomerization of (cyanomethylene)cyclopropane (**5**) into 1-cyano-2-methylenecyclopropane (7).[36]

Spectroscopy. The rotational spectrum of 1-cyano-2-methylenecyclopropane (7) was collected from 235 to 500 GHz using a previously described millimeter-wave spectrometer in a continuous flow at room temperature, with a sample pressure of 12 mTorr.[37−40] The complete spectrum from 235 to 500 GHz was obtained using automated data collection software in less than 2.5 days with the following experimental

Scheme 1. Synthesis of 1-Cyano-2-methylenecyclopropane (7)

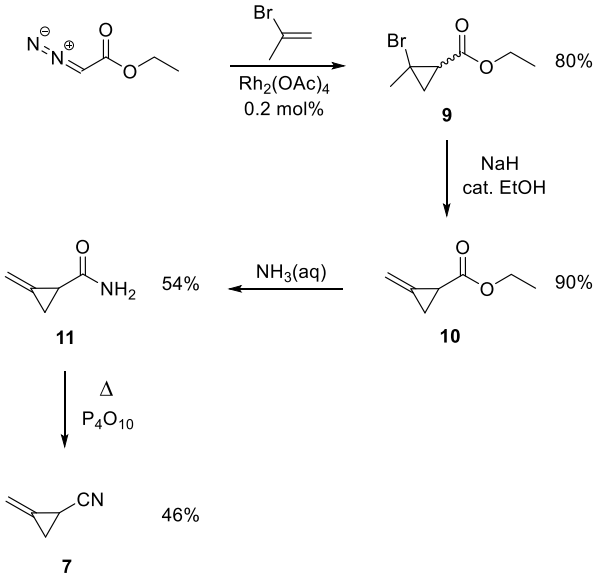

parameters: 0.6 MHz/s sweep rate, 10 ms time constant, and 50 kHz AM and 500 kHz FM modulation in a tone-burst design. The separate spectral segments were combined into a single broadband spectrum using Kisiel's Assignment and Analysis of Broadband Spectra (AABS) software.[41,42] Pickett's SPFIT/SPCAT was used for least-squares fitting and spectral predictions,[43] along with the PIFORM program for analysis.[44] A uniform frequency measurement uncertainty of 50 kHz was assumed for all measurements.

Computation. Electronic structure calculations were carried out with Gaussian 16[45] using the WebMO interface.[46] Optimized geometries were obtained with various levels of theory (including the MP2/cc-pVTZ level) using "VeryTight" convergence criteria and an "UltraFine" integration grid, and subsequently anharmonic vibrational calculations were carried out in Gaussian 16. The results of these calculations are discussed in the Supporting Information. Through the course of this investigation, it became clear that there were some issues with the computed spectroscopic values in the Gaussian output files. As a result, an optimized structure was obtained separately, using a development version of CFOUR,[47] at the MP2/cc-pVTZ level and subsequently used for a second-order vibrational perturbation (VPT2) anharmonic frequency calculation by evaluating the cubic force constants using analytical second derivatives at displaced points.[48−50] The anharmonic vibrational calculations provided computed rotational constants, quartic and sextic centrifugal distortion constants, and vibration−rotation interaction constants. All computational output files are provided in the Supporting Information. Only the MP2/cc-pVTZ-computed spectroscopic constants from CFOUR will be discussed in the remainder of this paper.

RESULTS AND DISCUSSION

Ground Vibrational State. The three large dipole moment components result in rotational spectra that contain many observable a-, b-, and c-type transitions. Figure 3 provides the complete predicted spectrum of 1-cyano-2-methylenecyclopropane (7) at frequencies up to 750 GHz at

https://doi.org/10.1021/acs.jpca.3c08002
J. Phys. Chem. A 2024, 128, 1427−1437

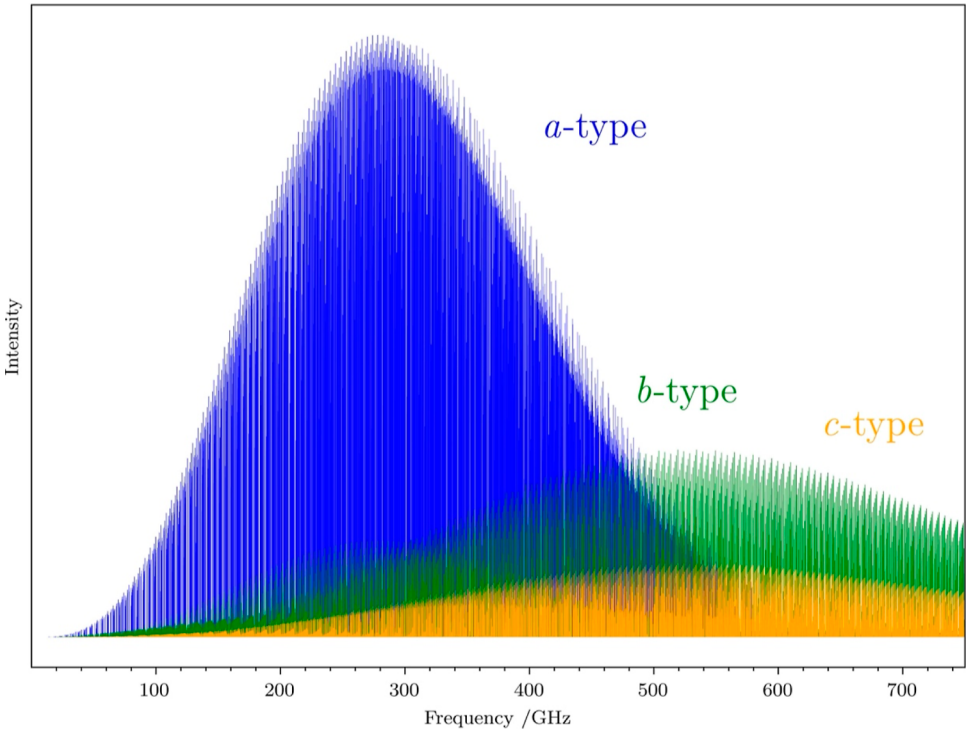

Figure 3. Predicted rotational spectrum of the ground vibrational state of 1-cyano-2-methylenecyclopropane (7) to 750 GHz at 292 K. *a*-Type transitions are displayed in blue, *b*-type transitions are displayed in green, and *c*-type transitions are displayed in yellow.

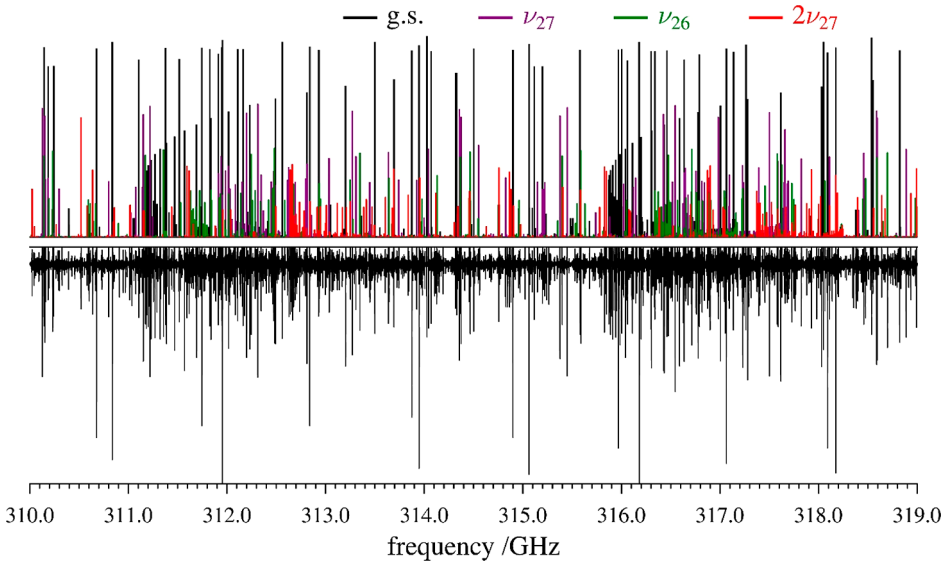

Figure 4. Predicted (top) and experimental (bottom) rotational spectra of 1-cyano-2-methylenecyclopropane (7) from 310.0 to 319.0 GHz. Ground-state transitions for the $J'' + 1 = 66$ and $J'' + 1 = 67$ bands appear in black, ν_{27} in purple, ν_{26} in green, and $2\nu_{27}$ in red.

292 K. The *a*-type ($\Delta K_a = 0$) transitions have their peak intensity at lower frequency, while the *b*- ($\Delta K_a = \pm 1$) and *c*-type ($\Delta K_a = \pm 1$) transitions have their intensity maximum at higher frequency. This circumstance allows for a much greater range of transition J and K energy levels in the same frequency range. In the spectral segment from 310 to 319 GHz shown in Figure 4, for example, the spectrum is dominated by intense *a*-type, $R_{0,1}$ transitions, which form prominent prolate-type band structures. These recognizable bands are those expected from a moderately prolate molecule, $\kappa = -0.846$, at high-J and high-K_a values. These bands are separated by approximately $B + C$ (~4.7 GHz). The $K_a = 0$ transitions for each band are located at much lower frequencies. For the $J'' + 1 = 67$ band shown in Figure 4, the $K_a = 0^+/1^-$ transition (K_c degenerate, oblate-type behavior) is 29.3 GHz lower in frequency than the main body of the band and appears as a degenerate set of two more-intense *a*-type and two less-intense *b*-type R-branch transitions. As K_a increases, the transitions progress to higher frequencies and eventually lose their K_a degeneracy, forming quartets of transitions (at $K_a = 7^+/8^-$ for the $J'' + 1 = 67$ band, asymmetric-top behavior). At moderate values of K_a ($K_a = 12^+$ for the $J'' + 1 = 67$ band), the transitions turn around and progress toward lower frequency with increasing K_a, eventually forming K_c degenerate pairs of *a*-type R-branch transitions (at

https://doi.org/10.1021/acs.jpca.3c08002
J. Phys. Chem. A 2024, 128, 1427−1437

Table 1. Spectroscopic Constants for the Ground Vibrational State of 1-Cyano-2-methylenecyclopropane (7) (S- and A-Reduced Hamiltonian, I^r Representation)

	S reduction, I^r representation			A reduction, I^r representation	
	experimental	MP2[a]		experimental	MP2[a]
$A_0^{(S)}$ (MHz)	7780.58024 (38)	7731	$A_0^{(A)}$ (MHz)	7780.57901 (39)	7731
$B_0^{(S)}$ (MHz)	2566.80795 (12)	2563	$B_0^{(A)}$ (MHz)	2566.81361 (12)	2563
$C_0^{(S)}$ (MHz)	2132.05792 (13)	2128	$C_0^{(A)}$ (MHz)	2132.05216 (13)	2128
D_J (kHz)	1.182678 (23)	1.188	Δ_J (kHz)	1.238500 (25)	1.243
D_{JK} (kHz)	−7.264766 (87)	−7.353	Δ_{JK} (kHz)	−7.60087 (13)	−7.679
D_K (kHz)	37.0123 (11)	36.66	Δ_K (kHz)	37.2913 (11)	36.93
d_1 (kHz)	−0.332432 (14)	−0.3333	δ_J (kHz)	0.332470 (14)	0.3333
d_2 (kHz)	−0.0279227 (71)	−0.02715	δ_K (kHz)	2.79381 (76)	2.704
H_J (Hz)	0.0031770 (26)	0.003170	Φ_J (Hz)	0.0038662 (34)	0.003880
H_{JK} (Hz)	−0.001669 (12)	−0.001445	Φ_{JK} (Hz)	0.010728 (99)	0.01137
H_{KJ} (Hz)	−0.164367 (52)	−0.1659	Φ_{KJ} (Hz)	−0.21721 (37)	−0.2192
H_K (Hz)	0.7200 (13)	0.7260	Φ_K (Hz)	0.7588 (14)	0.7659
h_1 (Hz)	0.0015011 (18)	0.001520	ϕ_J (Hz)	0.0015450 (18)	0.001563
h_2 (Hz)	0.0003449 (12)	0.0003550	ϕ_{JK} (Hz)	0.02201 (13)	0.02292
h_3 (Hz)	0.00004182 (26)	0.00004280	ϕ_K (Hz)	0.2825 (19)	0.2869
L_J (μHz)	−0.00000832 (10)		L_J (μHz)	−0.00001259 (16)	
L_{JJK} (μHz)	−0.00016332 (58)		L_{JJK} (μHz)	−0.0001628 (75)	
L_{JK} (μHz)	0.0012279 (33)		L_{JK} (μHz)	0.001246 (27)	
L_{KKJ} (μHz)	0.000102 (12)		L_{KKJ} (μHz)	0.000434 (21)	
L_K (μHz)	−0.00771 (54)		L_K (μHz)	−0.00767 (54)	
l_1 (μHz)	−0.000005039 (77)		l_J (μHz)	−0.000005363 (82)	
l_2 (μHz)	−0.000002107 (58)		l_{JK} (μHz)	−0.0000822 (59)	
l_3 (μHz)	−0.000000242 (19)		l_{KJ} (μHz)	0.00086 (14)	
l_4 (μHz)	[0.0][b]		l_K (μHz)	[0.0][b]	
N_{lines}[c]	3604		N_{lines}[c]	3604	
σ_{fit} (MHz)	0.041		σ_{fit} (MHz)	0.042	
κ[d]	−0.846065925 (61)	−0.889	κ[d]	−0.846062005 (61)	−0.889
Δ_i (μÅ^2)[e]	−24.805848 (17)	−34.3	Δ_i (μÅ^2)[e]	−24.804784 (17)	−34.3

[a]Calculated using the cc-pVTZ basis set in CFOUR. [b]Bracketed values held constant. [c]Number of independent transition frequencies. [d]$\kappa = (2B - A - C)/(A - C)$ using a custom script. [e]Inertial defect ($\Delta_i = I_c - I_a - I_b$) calculated from the B_0 constants using a custom script.

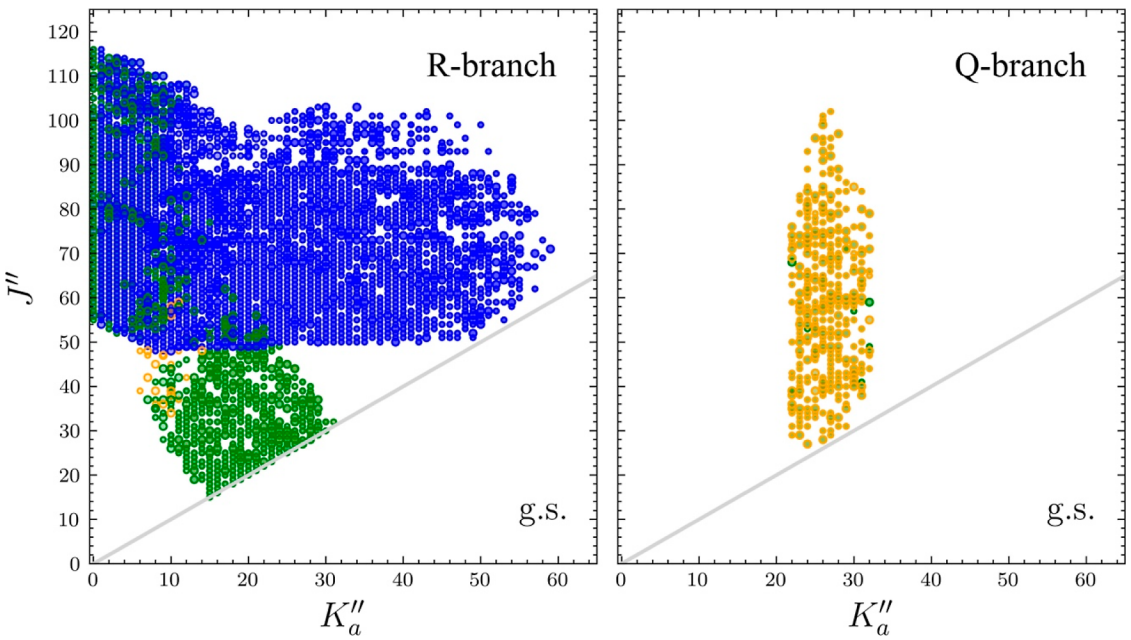

Figure 5. Data distribution plots for the least-squares fit of spectroscopic data for the vibrational ground state of 1-cyano-2-methylenecyclopropane (7). *a*-Type transitions are represented by blue circles, *b*-type transitions by green circles, and *c*-type transitions are represented by yellow circles. The size of the symbol is proportional to the value of $|(f_{obs.} - f_{calc.})/\delta f|$, where δf is the frequency measurement uncertainty and all values are smaller than 3.

https://doi.org/10.1021/acs.jpca.3c08002
J. Phys. Chem. A 2024, 128, 1427−1437

K_a = $18^+/18^-$ for the J'' + 1 = 67 band, true prolate-type behavior). In the J'' + 1 = 67 band, the R-branch series progresses to lower frequency until K_a = $34^+/34^-$, where the transitions form the distinct prolate-type bands, shown in Figure 4. This series turns around once again to progress toward higher frequencies with increasing K_a, until the transitions become lost in the spectral confusion as they become progressively less intense. For 1-cyano-2-methylenecyclopropane (7), these bands are highly overlapped with transitions of one band running through many others, visually obscuring the K_a = 0 band origins. Further complicating the initial transition assignments, similar spectral patterns are visible for many vibrationally excited states (including ν_{27}, ν_{26}, and $2\nu_{27}$), albeit with decreasing intensity as the vibrational energy increases. Due to the spectral density of the transitions from the ground and vibrationally excited states, the initial transition assignments relied heavily on computed rotational and centrifugal distortion constants. The initial predictions, combined with the use of Loomis–Wood plots of the predicted $^aR_{0,1}$ K_a = 0 series, were critical to begin the measurement, assignment, and least-squares fitting process. Once the initial assignments were made, progressing along the *a*-type series described above allowed for a rapid refinement of the spectroscopic constants and the accurate prediction and subsequent assignments of many more *a*-, *b*-, and *c*-type transitions.

In the end, more than 3600 independent transitions for the ground vibrational state have been measured, assigned, and least-squares fit to partial-octic, distorted-rotor Hamiltonians in both the A (σ_{fit} = 41 kHz) and S (σ_{fit} = 42 kHz) reductions. Although the data set is dominated by *a*-type transitions, the significant dipole components along the *b*- and *c*-axes result in a large number of *b*- and *c*-type transitions of both R- and Q-branch types. The large number of transitions, large frequency range, and number of nondegenerate *a*-, *b*-, and *c*-type transitions in the data set combine to provide a complete determination of the rotational constants and centrifugal distortion constants through the sextic level (Table 1). As shown in Figure 5, these transitions cover a large range of quantum numbers, from 15 to 117 for J'' and from 0 to 59 for K_a''. The computed spectroscopic constants (MP2/cc-pVTZ, CFOUR) are presented in Table 1, alongside their experimentally determined values. The computed rotational constants are all within 0.7% of their experimentally determined values. The MP2 quartic centrifugal distortion constants are in quite good agreement with the experimental values (within 1.2%), with only d_2 and δ_K displaying larger deviations (3.5%) from their experimentally determined values. Expectedly, the agreement between the computed sextic distortion constants and the experimental values is somewhat diminished but still quite good, with the computed values being within 6% of the experimental values, except for H_{JK}, which deviates by 13.4%. This is not dissimilar from the agreement that was found in our related work on (cyanomethylene)cyclopropane (5), the closely related isomer.[5] All of the constants are needed to achieve a satisfactory fit. The likelihood that all of the experimentally determined values are physically meaningful will be further supported by the analysis of the fitted constants across the v ν_{27} series (*vide infra*). That the centrifugal distortion constants with the worst agreement with their experimental counterparts include all of the J/K-dependent, sextic centrifugal distortion constants in both the A and S reduction suggests a systematic, albeit small, issue with the computed geometry or cubic force constants. All octic distortion constants, except l_4 and l_k, were successfully determined. The values of l_4 and l_k were held constant at zero in the least-squares fit, as computed values are not available for the octic centrifugal distortion constants. The lack of a computational comparison also makes it more difficult to judge the physical meaningfulness of the octic distortion constants.

Vibrationally Excited States (ν_{27}, ν_{26}, and $2\nu_{27}$). The vibrational energy manifold of 1-cyano-2-methylenecyclopropane (7) below 500 cm^{-1}, which includes the vibrationally excited states analyzed in this work (ν_{27}, ν_{26}, and $2\nu_{27}$), is shown in Figure 6. Even though many of the higher-energy states were sufficiently intense to identify in the spectral data, this work focuses on the two fundamental and the first overtone states, all of which could be treated with single-state, distorted-rotor Hamiltonians. We believe that the higher-energy vibrational states form Coriolis- and anharmonic-coupled polyads based upon our observation of perturbations of their transition frequencies. The complete analysis of these other vibrationally excited states is beyond the scope of the current work.

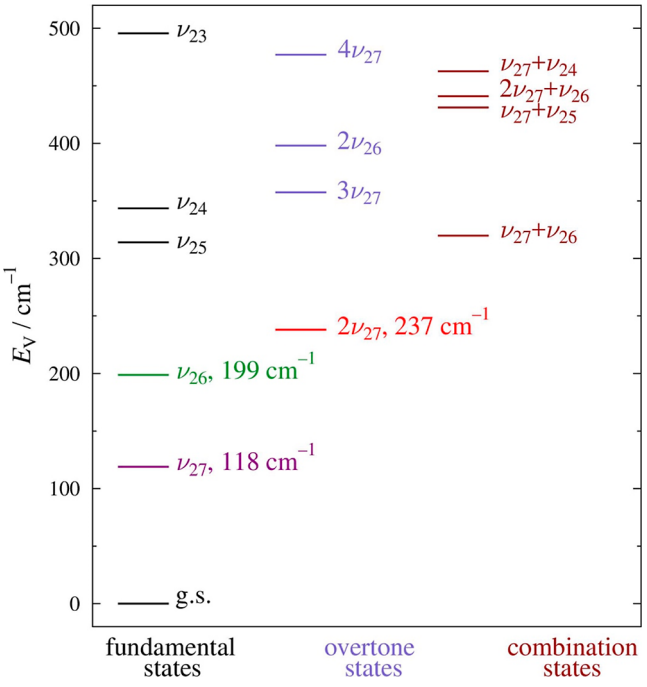

Figure 6. Vibrational energy levels of 1-cyano-2-methylenecyclopropane (7) below 500 cm^{-1} from computed fundamental frequencies (MP2/cc-pVTZ). All states are of *A* symmetry.

The lowest-energy fundamental, ν_{27} (*A*, 118 cm^{-1}, MP2), involves a symmetric scissor motion of the nitrile and exocyclic methylene groups. The next lowest-energy fundamental, ν_{26} (*A*, 199 cm^{-1}), is best described as a nitrile bending vibration. The lowest-energy overtone is $2\nu_{27}$ (*A*, 237 cm^{-1}), which is less than 50 cm^{-1} higher in energy than ν_{26}. Utilizing the experimental centrifugal distortion constants from the ground state and correcting the ground-state rotational constants with the computed vibration–rotation interaction constants (B_0-B_v) [using either B3LYP/6-311+G(2d,p) or MP2/6-311+G(2d,p) in Gaussian 16] provided surprisingly good initial predictions (*vide infra*) of the ν_{27} and ν_{26} spectra. The poor

https://doi.org/10.1021/acs.jpca.3c08002
J. Phys. Chem. A 2024, 128, 1427–1437

Table 2. Spectroscopic Constants for the Ground and Three Lowest-Energy Vibrationally Excited States of 1-Cyano-2-methylenecyclopropane (7) (S-Reduced Hamiltonian, I′ Representation)

	g.s.	ν_{27} (118 cm^{-1})[a]	ν_{26} (199 cm^{-1})[a]	$2\nu_{27}$ (237 cm^{-1})[a]
$A_v^{(S)}$ (MHz)	7780.58024 (38)	7795.9069 (78)	7785.7914 (97)	7811.1669 (91)
$B_v^{(S)}$ (MHz)	2566.80795 (12)	2575.55474 (47)	2570.02452 (59)	2584.25774 (60)
$C_v^{(S)}$ (MHz)	2132.05792 (13)	2134.39410 (34)	2135.70106 (42)	2136.66803 (45)
D_J (kHz)	1.182678 (23)	1.185238 (50)	1.188216 (65)	1.187597 (73)
D_{JK} (kHz)	−7.264766 (87)	−7.11284 (25)	−7.38331 (33)	−6.96318 (33)
D_K (kHz)	37.0123 (11)	36.940 (33)	37.299 (39)	36.766 (23)
d_1 (kHz)	−0.332432 (14)	−0.338241 (43)	−0.333450 (54)	−0.343878 (52)
d_2 (kHz)	−0.0279227 (71)	−0.030752 (14)	−0.027517 (16)	−0.033629 (10)
H_J (Hz)	0.0031770 (26)	0.0031137 (57)	0.0031522 (74)	0.0030552 (88)
H_{JK} (Hz)	−0.001669 (12)	−0.001779 (98)	−0.00179 (12)	−0.002116 (55)
H_{KJ} (Hz)	−0.164367 (52)	−0.15923 (36)	−0.16803 (39)	−0.15426 (15)
H_K (Hz)	0.7200 (13)	1.047 (50)	0.856 (60)	[1.374][b]
h_1 (Hz)	0.0015011 (18)	0.0015080 (48)	0.0014812 (61)	0.0014999 (60)
h_2 (Hz)	0.0003449 (12)	0.0003671 (20)	0.0003476 (24)	0.00038914 (92)
h_3 (Hz)	0.00004182 (26)	0.00004663 (20)	0.00004258 (21)	0.00005518 (82)
L_J (μHz)	−0.00000832 (10)	−0.00000726 (25)	−0.00000630 (31)	−0.00000635 (41)
L_{JJK} (μHz)	−0.00016332 (58)	−0.0001582 (21)	−0.0001710 (28)	−0.0001448 (34)
L_{JK} (μHz)	0.0012279 (33)	0.001176 (12)	0.001246 (14)	0.001167 (14)
L_{KKJ} (μHz)	0.000102 (12)	[0.000102][b]	[0.000102][b]	[0.000102][b]
L_K (μHz)	−0.00771 (54)	[−0.00771][b]	[−0.00771][b]	[−0.00771][b]
l_1 (μHz)	−0.000005039 (77)	−0.00000489 (20)	−0.00000365 (26)	−0.00000434 (27)
l_2 (μHz)	−0.000002107 (58)	−0.000002201 (98)	−0.00000219 (11)	[−0.000002295] [b]
l_3 (μHz)	−0.000000242 (19)	[−0.000000242] [b]	[−0.000000242] [b]	−0.000000320 (51)
l_4 (μHz)	[0.0][b]	[0.0][b]	[0.0][b]	[0.0][b]
N_{lines}[c]	3604	1958	1475	1409
σ_{fit} (MHz)	0.041	0.039	0.041	0.040
κ[d]	−0.846065925 (61)	−0.84415450 (29)	−0.84625983 (39)	−0.84224520 (36)
Δ_i (μÅ^2)[e]	−24.805848 (17)	−24.268943 (83)	−24.91996 (11)	−23.73347 (10)

[a]Vibrational energy calculated at the MP2/cc-pVTZ level in CFOUR. [b]Bracketed values held constant at zero, at their respective ground-state value, or at a value extrapolated from lower-energy vibrational states using an appropriate polynomial. [c]Number of independent transition frequencies. [d]$\kappa = (2B - A - C)/(A - C)$, using a custom script. [e]Inertial defect ($\Delta_i = I_c - I_a - I_b$) calculated from the B_v constants using a custom script.

agreement between the computed (Gaussian 16) and experimental vibration−rotation interaction constants subsequently obtained from the least-squares fits of ν_{27} and ν_{26} was a key observation that led us to identify an error in the computed values (Supporting Information). The initial prediction of the $2\nu_{27}$ spectrum was made using the linear extrapolation of ground-state and ν_{27} spectroscopic constants. The good predictions of the spectra for all of these states made the initial assignment, measurement, and least-squares fitting quite straightforward, despite the spectral density. In the final least-squares fits, centrifugal distortion constants that could not be determined were held constant at the corresponding ground-state values (or extrapolated values in the case of $2\nu_{27}$). The range of measured transition frequencies and associated quantum numbers included in the analysis for these vibrationally excited states is only slightly reduced relative to the ground vibrational state. No *c*-type transitions, however, could be assigned and measured for these states, due to their lower populations. The final data set for ν_{27} included over 1900 transitions least-squares fit to both A- and S-reduced, partial-octic, distorted-rotor Hamiltonians, with low error (σ_{fit} = 39 kHz). Similarly, the final data sets for ν_{26} and $2\nu_{27}$ included over 1400 transitions each, fit to both A- and S-reduced, partial-octic, distorted-rotor Hamiltonians, with comparably low error (ν_{26}, σ_{fit} = 41 kHz; $2\nu_{27}$, σ_{fit} = 40 kHz). The resulting S-reduction spectroscopic constants are presented in Table 2 along with the ground-state constants for a convenient comparison. The data distribution plots and A-reduction spectroscopic constants are available in the Supporting Information.

The computed (CFOUR) and experimental vibration−rotation interaction constants (B_0−B_v) for ν_{27} and ν_{26} are provided in Table 3, as well as the experimental values of $2\nu_{27}$ for comparison. The relative intensity of the transitions and a comparison of the computed and experimental vibration−

Table 3. Experimental and Computed Vibration−Rotation Interaction Constants for 1-Cyano-2-methylenecyclopropane (7)

	experimental	MP2[a]	obs.−calc.
A_0−A_{27} (MHz)	−15.3267 (78)	−16.06	0.751
B_0−B_{27} (MHz)	−8.74679 (49)	−8.678	−0.069
C_0−C_{27} (MHz)	−2.33618 (36)	−2.279	−0.057
A_0−A_{26} (MHz)	−5.23576 (40)	−6.302	1.069
B_0−B_{26} (MHz)	−3.21733 (61)	−3.272	0.055
C_0−C_{26} (MHz)	−3.64248 (45)	−3.743	0.101
$A_0 - A_{2\nu_{27}}$ (MHz)	−30.58467 (91)		
$B_0 - B_{2\nu_{27}}$ (MHz)	−17.44979 (61)		
$C_0 - C_{2\nu_{27}}$ (MHz)	−4.61011 (47)		

[a]Evaluated with the cc-pVTZ basis set in CFOUR.

https://doi.org/10.1021/acs.jpca.3c08002
J. Phys. Chem. A 2024, 128, 1427−1437

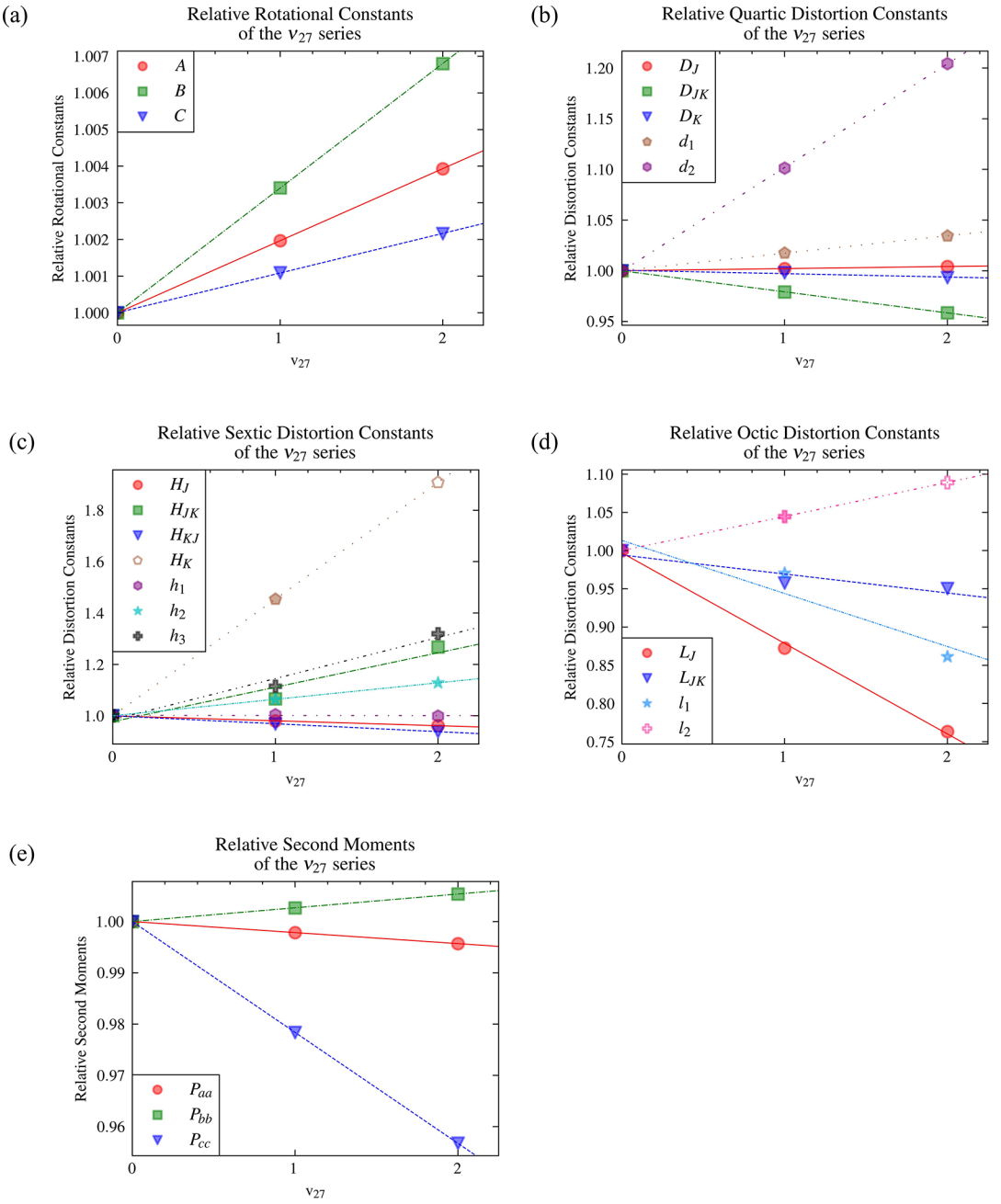

Figure 7. (a) Relative rotational constants, (b) relative quartic centrifugal distortion constants, (c) relative sextic distortion constants, (d) relative octic distortion constants, and (e) relative second moments for 1-cyano-2-methylenecyclopropane (7) as a function of vibrational excitation (v ν_{27}, where v = 0, 1, 2). Open symbols represent values fixed in the least-squares fits to those extrapolated from the lower-energy states in the vibrational sequence.

rotation constants make the assignment of ν_{27}, ν_{26}, and $2\nu_{27}$ unambiguous. The agreement between computed and experimental constants is excellent, with little deviation for ν_{27} and ν_{26}. Similarly, the vibration−rotation interaction constants for $2\nu_{27}$ demonstrate a linear relationship to the fundamental. The vibration−rotation interaction constants (A_0−A_v and B_0−B_v) for ν_{26} are smaller than those for ν_{27}. The origin of this difference is likely associated with the difference in vibrational motion between the two modes. In ν_{27}, the scissoring motion of the nitrile and exocyclic methylene groups causes those groups to move further from the *a*- and *b*-axes, whereas in ν_{26}, only the nitrile group bends, which has a smaller impact on the A_v and B_v values. Collectively, these observations provide support for the physical meaningfulness of the spectroscopic constants, determined for both the ground state and the excited vibrational states, as well as the appropriateness of the use of a single-state Hamiltonian model for each. As will be described below, the reliability of these spectroscopic constants also provides an important benchmark for computational chemistry software.

For all three vibrationally excited states (ν_{27}, ν_{26}, and $2\nu_{27}$), a full set of quartic and sextic centrifugal distortion constants has been determined for the A and S reduction, except for H_K of $2\nu_{27}$ (Table 2). As expected, the number of octic centrifugal distortion constants that could be satisfactorily determined by least-squares fitting decreased as the vibrational energy

https://doi.org/10.1021/acs.jpca.3c08002
J. Phys. Chem. A 2024, 128, 1427−1437

increased, primarily due to the decrease in the number of transitions included in the data set. The quartic centrifugal distortion constants of fundamental vibrational states ν_{27} and ν_{26} show the expected small deviations (<10%) in centrifugal distortion from the ground state. The sextic centrifugal distortion constants show greater deviations, with H_K and h_3 changing by 48 and 15%, respectively. The spectroscopic constants of $2\nu_{27}$ are quite similar to those expected by linear extrapolation from the ground state and ν_{27}, which will be discussed in detail below. The close agreement between the centrifugal distortion constants for the vibrationally excited states and those of the ground vibrational state suggests that these values, particularly the quartic constants, should provide good experimental benchmarks for future computational predictions.

Analysis of $v\,\nu_{27}$ (v = 0, 1, and 2) Series. The robust data set derived from the current experimental measurements of the ground state, ν_{27}, and $2\nu_{27}$ of 1-cyano-2-methylenecyclopropane (7) allows a more rigorous analysis of the spectroscopic constants for each species. If all of the experimental spectroscopic constants determined by least-squares fitting are physically meaningful, the variation of the spectroscopic constants across the v ν_{27} series should be smooth and nearly linear.[51−56] In Figure 7, each of the spectroscopic constants is plotted as a function of ν_{27} along with a linear trendline model. Constants were included only when two or more values were experimentally determined to be able to fit a linear regression model to the experimental data. Open symbols represent fixed constants that were not determined in the least-squares fitting process. Figure 7a,e shows the minimal deviation from linearity in the relative rotational constants and resulting second moments across the series. The relative deviation from the extrapolated value is less than 0.4% for each constant. Similarly, Figure 7b−d shows the relative centrifugal distortion constants across the v ν_{27} series. The quartic centrifugal distortion constants also vary linearly with vibrational excitation. The smooth linear progression of the quartic distortion constants provides unambiguous confirmation that all of them are physically meaningful and are well-determined in the least-squares fits. The sextic centrifugal distortion constants demonstrate a linear trend. Of the seven sextic distortion constants for each of the three vibrational states of 7 (v ν_{27}, v = 0, 1, and 2), the only constant that is not determinable in the least-squares fits is the term H_K for $2\nu_{27}$. Holding the value of the H_K constant at the extrapolated value depicted in Figure 7c, however, provides a satisfactory least-squares fit for $2\nu_{27}$. That the remaining sextic, as well as the octic, centrifugal distortion constants display the expected linearity suggests that the extrapolated value of H_K is a reasonable estimate of its actual value and that the values of the remaining constants are physically meaningful. The octic centrifugal distortion constants that are determinable in the current study demonstrate a smooth dependence on vibrational excitation (Figure 7d), although the plots are slightly less smooth and with greater deviation from linearity than the quartic or sextic centrifugal distortion constants. To the best of our knowledge, this is the first time that such an analysis has been carried out on the octic constants of any molecule. The near linearity suggests that the octic distortion constants are as physically meaningful as they can be given that some of the octic terms were held constant at zero.

Analysis of the Computational Results. As discussed above, the agreement between the computed (CFOUR) spectroscopic constants and those determined experimentally is excellent. In the course of this work, we identified (and describe in detail in the Supporting Information) previously unreported issues with the computed spectroscopic constants reported in Gaussian 16. The spectroscopic constants are reported in a representation different from what the output representation label indicates (issue #1). The computational output files from Gaussian 16 indicate that the centrifugal distortion constants are in the III^r representation, though they are actually I^r. This has been confirmed by comparison to the experimental values and by direct calculation of the A- and S-reduction quartic centrifugal distortion constants from the τ distortion constants using the equations in Tables 8.14 and 8.16 in Gordy and Cook.[57] The S-reduction spectroscopic constant H_{JK} is computed to have the wrong sign and magnitude for molecules of C_1 symmetry (issue #2). This is particularly problematic given the increased need for the inclusion of sextic centrifugal distortion in least-squares fits due to the increased prevalence of wide-frequency-range millimeter-wave spectrometers. While all of the A-reduction spectroscopic constants are well-predicted, the generation of reliable computed constants in the S reduction is also important, as the A reduction is known to break down for molecules that are highly prolate, oblate, or spherical.[58−64] Finally, the previously reported issue in determining the vibration−rotation interaction constants[65] appears to not have been addressed for molecules of C_1 symmetry (issue #3). To the best of our knowledge, this is the first report of these issues.

CONCLUSIONS

The rotational transitions of 1-cyano-2-methylenecyclopropane (7), a newly synthesized isomer of pyridine, are available for the first time. Combined with its companion work, the analysis of 7 herein provides a near-complete spectroscopic characterization of this new compound.[36] The large number of transitions (over 3600) across a 265 GHz frequency range, covering transitions with over 100 J energy levels, affords a satisfactory determination of a nearly full set of spectroscopic constants through the octic level of centrifugal distortion. These spectroscopic constants are likely to predict the spectrum well outside the observed frequency range due to the inclusion of a-, b-, and c-type transitions in the data set and the types of transitions that will be encountered in new frequency ranges. The higher-frequency spectrum of 7 (>500 GHz) will be dominated by b- and c-type transitions whose energy levels are already well-described by the spectroscopic constants because there are a-type transitions in the data set with those energy levels. Likewise, the lower-frequency spectrum of 7 (<235 GHz) will be dominated by a-type transitions with energy levels already included in the data set for b- and c-type transitions. Combined with computed or experimental nuclear quadrupole coupling constants, these constants should adequately predict all of the rotational transitions available to current radiotelescopes.

Meaningful analysis and prediction of experimental rotational spectra require the availability of reliable computational prediction of spectroscopic parameters. Detailed studies of the ground and vibrationally excited states of molecules over a wide range of frequencies and quantum numbers, in turn, provide new benchmarks for computational predictions. This study provides spectroscopic constants for two fundamental vibrational states that can be used as benchmarks for the future development of computational methods. Despite some recent

https://doi.org/10.1021/acs.jpca.3c08002
J. Phys. Chem. A 2024, 128, 1427−1437

advances,[66−72] very few studies have included computational prediction of the centrifugal distortion of vibrationally excited states. In addition, we unintentionally provided a benchmark for the existing computational software. The uncovered issues in Gaussian 16 make it more difficult to make accurate initial predictions of the rotational spectra for C_1 molecules in the ground and excited vibrational states. These issues may cause spectroscopists to question the physical meaning of obtained rotational constants that are quite different than their theoretical predictions, as that disagreement can be a sign of unaddressed coupling between vibrational states. We are hopeful that these issues will be addressed in the future given the widespread use of Gaussian 16 by the spectroscopic community and its relative ease of use for most experimental chemists.

■ ASSOCIATED CONTENT

Supporting Information

The Supporting Information is available free of charge at https://pubs.acs.org/doi/10.1021/acs.jpca.3c08002.

Excited-state spectroscopic constants in the A reduction, detailed discussion of Gaussian 16 predictions, and data distribution plots (PDF)

Computational output files and least-squares fitting output files from SPFIT (ZIP)

■ AUTHOR INFORMATION

Corresponding Authors

R. Claude Woods − *Department of Chemistry, University of Wisconsin−Madison, Madison, Wisconsin 53706-1322, United States;* orcid.org/0000-0003-0865-4693; Email: rcwoods@wisc.edu

Robert J. McMahon − *Department of Chemistry, University of Wisconsin−Madison, Madison, Wisconsin 53706-1322, United States;* orcid.org/0000-0003-1377-5107; Email: robert.mcmahon@wisc.edu

Authors

Dairen R. Jean − *Department of Chemistry, University of Wisconsin−Madison, Madison, Wisconsin 53706-1322, United States*

Samuel A. Wood − *Department of Chemistry, University of Wisconsin−Madison, Madison, Wisconsin 53706-1322, United States*

Brian J. Esselman − *Department of Chemistry, University of Wisconsin−Madison, Madison, Wisconsin 53706-1322, United States;* orcid.org/0000-0002-9385-8078

Complete contact information is available at: https://pubs.acs.org/10.1021/acs.jpca.3c08002

Notes

The authors declare no competing financial interest.

■ ACKNOWLEDGMENTS

We gratefully acknowledge the National Science Foundation for its support of this project (CHE-1954270). D.R.J. thanks the Department of Chemistry and Life Science, United States Military Academy, for graduate education funding.

■ REFERENCES

(1) McGuire, B. A. 2021 Census of Interstellar, Circumstellar, Extragalactic, Protoplanetary Disk, and Exoplanetary Molecules. *Astrophys. J. Suppl.* **2022**, *259*, 30.

(2) Endres, C. P.; Schlemmer, S.; Schilke, P.; Stutzki, J.; Müller, H. S. The Cologne Database for Molecular Spectroscopy, CDMS, in the Virtual Atomic and Molecular Data Centre, VAMDC. *J. Mol. Spectrosc.* **2016**, *327*, 95−104.

(3) Dorman, P. M.; Esselman, B. J.; Changala, P. B.; Kougias, S. M.; McCarthy, M. C.; Woods, R. C.; McMahon, R. J. Rotational spectrum of *anti*- and *gauche*-4-cyano-1-butyne (C_5H_5N) - An open-chain isomer of pyridine. *J. Mol. Spectrosc.* **2022**, *385*, 111604.

(4) Esselman, B. J.; Kougias, S. M.; Fellows, M. D.; Woods, R. C.; McMahon, R. J. The 130−360 GHz rotational spectrum of isocyanocyclobutane (C_4H_7NC) and cyanocyclobutane (C_4H_7CN). *J. Mol. Spectrosc.* **2022**, *388*, 111684.

(5) Esselman, B. J.; Kougias, S. M.; Zdanovskaia, M. A.; Woods, R. C.; McMahon, R. J. Synthesis, Purification, and Rotational Spectroscopy of (Cyanomethylene)Cyclopropane-An Isomer of Pyridine. *J. Phys. Chem. A* **2021**, *125*, 5601−5614.

(6) Zdanovskaia, M. A.; Dorman, P. M.; Orr, V. L.; Owen, A. N.; Kougias, S. M.; Esselman, B. J.; Woods, R. C.; McMahon, R. J. Rotational Spectra of Three Cyanobutadiene Isomers (C_5H_5N) of Relevance to Astrochemistry and Other Harsh Reaction Environments. *J. Am. Chem. Soc.* **2021**, *143*, 9551−9564.

(7) Zdanovskaia, M. A.; Esselman, B. J.; Kougias, S. M.; Patel, A. R.; Woods, R. C.; McMahon, R. J. The 130−360 GHz rotational spectrum of *syn*-2-cyano-1,3-butadiene (C_5H_5N) - a molecule of astrochemical relevance. *Mol. Phys.* **2021**, *119*, No. e1964629.

(8) Smith, H. H.; Kougias, S. M.; Esselman, B. J.; Woods, R. C.; McMahon, R. J. Synthesis, Purification, and Rotational Spectroscopy of 1-Cyanocyclobutene (C_5H_5N). *J. Phys. Chem. A* **2022**, *126*, 1980−1993.

(9) Dorman, P. M.; Esselman, B. J.; Woods, R. C.; McMahon, R. J. An Analysis of the Rotational Ground State and Lowest-Energy Vibrationally Excited Dyad of 3-Cyanopyridine: Low Symmetry Reveals Rich Complexity of Perturbations, Couplings, and Interstate Transitions. *J. Mol. Spectrosc.* **2020**, *373*, 111373.

(10) Zdanovskaia, M. A.; Esselman, B. J.; Lau, H. S.; Bates, D. M.; Woods, R. C.; McMahon, R. J.; Kisiel, Z. The 103 - 360 GHz Rotational Spectrum of Benzonitrile, the First Interstellar Benzene Derivative Detected by Radioastronomy. *J. Mol. Spectrosc.* **2018**, *351*, 39−48.

(11) Zdanovskaia, M. A.; Martin-Drumel, M.-A.; Kisiel, Z.; Pirali, O.; Esselman, B. J.; Woods, R. C.; McMahon, R. J. The eight lowest-energy vibrational states of benzonitrile: analysis of Coriolis and Darling-Dennison couplings by millimeter-wave and far-infrared spectroscopy. *J. Mol. Spectrosc.* **2022**, *383*, 111568.

(12) Smith, H. H.; Esselman, B. J.; Zdanovskaia, M. A.; Woods, R. C.; McMahon, R. J. The 130−500 GHz rotational spectrum of 2-cyanopyrimidine. *J. Mol. Spectrosc.* **2023**, *391*, 111737.

(13) Dorman, P. M.; Esselman, B. J.; Park, J. E.; Woods, R. C.; McMahon, R. J. Millimeter-Wave Spectrum of 4-Cyanopyridine in its Ground State and Lowest Energy Vibrationally Excited States, ν_{20} and ν_{30}. *J. Mol. Spectrosc.* **2020**, *369*, 111274.

(14) Esselman, B. J.; Zdanovskaia, M. A.; Styers, W. H.; Owen, A. N.; Kougias, S. M.; Billinghurst, B. E.; Zhao, J.; Woods, R. C.; McMahon, R. J. Millimeter-Wave and High-Resolution Infrared Spectroscopy of 2-Furonitrile—A Highly Polar Substituted Furan. *J. Phys. Chem. A* **2023**, *127*, 1909−1922.

(15) Barnum, T. J.; Siebert, M. A.; Lee, K. L. K.; Loomis, R. A.; Changala, P. B.; Charnley, S. B.; Sita, M. L.; Xue, C.; Remijan, A. J.; Burkhardt, A. M.; et al. A Search for Heterocycles in GOTHAM Observations of TMC-1. *J. Phys. Chem. A* **2022**, *126*, 2716−2728.

(16) Simon, M. N.; Simon, M. Search for Interstellar Acrylonitrile, Pyrimidine, and Pyridine. *Astrophys. J.* **1973**, *184*, 757−761.

(17) McGuire, B. A.; Burkhardt, A. M.; Kalenskii, S.; Shingledecker, C. N.; Remijan, A. J.; Herbst, E.; McCarthy, M. C. Detection of the

aromatic molecule benzonitrile (*c*-C_6H_5CN) in the interstellar medium. *Science* **2018**, *359*, 202−205.
(18) McCarthy, M. C.; McGuire, B. A. Aromatics and Cyclic Molecules in Molecular Clouds: A New Dimension of Interstellar Organic Chemistry. *J. Phys. Chem. A* **2021**, *125*, 3231−3243.
(19) Lovas, F. J.; McMahon, R. J.; Grabow, J.-U.; Schnell, M.; Mack, J.; Scott, L. T.; Kuczkowski, R. L. Interstellar Chemistry: A Strategy for Detecting Polycyclic Aromatic Hydrocarbons in Space. *J. Am. Chem. Soc.* **2005**, *127*, 4345−4349.
(20) Lattelais, M.; Ellinger, Y.; Matrane, A.; Guillemin, J.-C. Looking for heteroaromatic rings and related isomers as interstellar candidates. *Phys. Chem. Chem. Phys.* **2010**, *12*, 4165−4171.
(21) Charnley, S. B.; Kuan, Y.-J.; Huang, H.-C.; Botta, O.; Butner, H. M.; Cox, N.; Despois, D.; Ehrenfreund, P.; Kisiel, Z.; Lee, Y.-Y.; et al. Astronomical searches for nitrogen heterocycles. *Adv. Space Res.* **2005**, *36*, 137−145.
(22) Etim, E. E.; Adelagun, R. O. A.; Andrew, C.; Enock Oluwole, O. Optimizing the searches for interstellar heterocycles. *Adv. Space Res.* **2021**, *68*, 3508−3520.
(23) Kutner, M. L.; Machnik, D. E.; Tucker, K. D.; Dickman, R. L. Search for interstellar pyrrole and furan. *Astrophys. J.* **1980**, *242*, 541−544.
(24) Cooke, I. R.; Xue, C.; Changala, P. B.; Shay, H. T.; Byrne, A. N.; Tang, Q. Y.; Fried, Z. T. P.; Kelvin Lee, K. L.; Loomis, R. A.; Lamberts, T.; et al. Detection of Interstellar *E*-1-cyano-1,3-butadiene in GOTHAM Observations of TMC-1. *Astrophys. J.* **2023**, *948*, 133.
(25) Kougias, S. M.; Knezz, S. N.; Owen, A. N.; Sanchez, R. A.; Hyland, G. E.; Lee, D. J.; Patel, A. R.; Esselman, B. J.; Woods, R. C.; McMahon, R. J. Synthesis and Characterization of Cyanobutadiene Isomers—Molecules of Astrochemical Significance. *J. Org. Chem.* **2020**, *85*, 5787−5798.
(26) Ye, E.; Bettens, R. P. A.; De Lucia, F. C.; Petkie, D. T.; Albert, S. Millimeter and submillimeter wave rotational spectrum of pyridine in the ground and excited vibrational states. *J. Mol. Spectrosc.* **2005**, *232*, 61−65.
(27) Thaddeus, P.; Vrtilek, J. M.; Gottlieb, C. A. Laboratory and Astronomical Identification of Cyclopropenylidene, C_3H_2. *Astrophys. J.* **1985**, *299*, L63−L66.
(28) Thaddeus, P.; Gottlieb, C. A.; Hjalmarson, A.; Johansson, L. E. B.; Irvine, W. M.; Friberg, P.; Linke, R. A. Astronomical Identification of the C_3H Radical. *Astrophys. J.* **1985**, *294*, L49−L53.
(29) Yamamoto, S.; Saito, S.; Ohishi, M.; Suzuki, H.; Ishikawa, S.-I.; Kaifu, N.; Murakami, A. Laboratory and Astronomical Detection of the Cyclic C_3H Radical. *Astrophys. J.* **1987**, *322*, L55−L58.
(30) Cernicharo, J.; Agúndez, M.; Cabezas, C.; Tercero, B.; Marcelino, N.; Pardo, J. R.; de Vicente, P. Pure hydrocarbon cycles in TMC-1: Discovery of ethynyl cyclopropenylidene, cyclopentadiene, and indene. *Astron. Astrophys.* **2021**, *649*, L15.
(31) Hollis, J. M.; Remijan, A. J.; Jewell, P. R.; Lovas, F. J. Cyclopropenone (*c*-H_2C_3O): A New Interstellar Ring Molecule. *Astrophys. J.* **2006**, *642*, 933−939.
(32) Dickens, J. E.; Irvine, W. M.; Ohishi, M.; Ikeda, M.; Ishikawa, S.; Nummelin, A.; Hjalmarson, Å. Detection of Interstellar Ethylene Oxide (*c*-C_2H_4O). *Astrophys. J.* **1997**, *489*, 753−757.
(33) Lykke, J. M.; Coutens, A.; Jørgensen, J. K.; van der Wiel, M. H. D.; Garrod, R. T.; Müller, H. S. P.; Bjerkeli, P.; Bourke, T. L.; Calcutt, H.; Drozdovskaya, M. N.; et al. The ALMA-PILS survey: First detections of ethylene oxide, acetone and propanal toward the low-mass protostar IRAS 16293−2422. *Astron. Astrophys.* **2017**, *597*, A53.
(34) McGuire, B. A.; Carroll, P. B.; Loomis, R. A.; Finneran, I. A.; Jewell, P. R.; Remijan, A. J.; Blake, G. A. Discovery of the interstellar chiral molecule propylene oxide (CH_3CHCH_2O). *Science* **2016**, *352*, 1449−1452.
(35) Apponi, A. J.; McCarthy, M. C.; Gottlieb, C. A.; Thaddeus, P. Astronomical Detection of Rhomboidal SiC_3. *Astrophys. J.* **1999**, *516*, L103−L106.
(36) Wood, S. A.; Esselman, B. J.; Kougias, S. M.; Woods, R. C.; McMahon, R. J. Photoisomerization of (Cyanomethylene)-cyclopropane (C_5H_5N) to 1-Cyano-2-methylenecyclopropane in an Argon Matrix. *J. Phys. Chem. A* **2024**, *128*, DOI: 10.1021/acs.jpca.3c08001.
(37) Amberger, B. K.; Esselman, B. J.; Stanton, J. F.; Woods, R. C.; McMahon, R. J. Precise Equilibrium Structure Determination of Hydrazoic Acid (HN_3) by Millimeter-wave Spectroscopy. *J. Chem. Phys.* **2015**, *143*, 104310.
(38) Esselman, B. J.; Amberger, B. K.; Shutter, J. D.; Daane, M. A.; Stanton, J. F.; Woods, R. C.; McMahon, R. J. Rotational Spectroscopy of Pyridazine and its Isotopologs from 235−360 GHz: Equilibrium Structure and Vibrational Satellites. *J. Chem. Phys.* **2013**, *139*, 224304.
(39) Zdanovskaia, M. A.; Esselman, B. J.; Woods, R. C.; McMahon, R. J. The 130 - 370 GHz Rotational Spectrum of Phenyl Isocyanide (C_6H_5NC). *J. Chem. Phys.* **2019**, *151*, 024301.
(40) Smith, H. H.; Esselman, B. J.; Wood, S. A.; Stanton, J. F.; Woods, R. C.; McMahon, R. J. Improved semi-experimental equilibrium structure and high-level theoretical structures of ketene. *J. Chem. Phys.* **2023**, *158*, 244304.
(41) Kisiel, Z.; Pszczółkowski, L.; Drouin, B. J.; Brauer, C. S.; Yu, S.; Pearson, J. C.; Medvedev, I. R.; Fortman, S.; Neese, C. Broadband Rotational Spectroscopy of Acrylonitrile: Vibrational Energies from Perturbations. *J. Mol. Spectrosc.* **2012**, *280*, 134−144.
(42) Kisiel, Z.; Pszczółkowski, L.; Medvedev, I. R.; Winnewisser, M.; De Lucia, F. C.; Herbst, E. Rotational Spectrum of *trans-trans* Diethyl Ether in the Ground and Three Excited Vibrational States. *J. Mol. Spectrosc.* **2005**, *233*, 231−243.
(43) Pickett, H. M. The fitting and prediction of vibration-rotation spectra with spin interactions. *J. Mol. Spectrosc.* **1991**, *148*, 371−377.
(44) Kisiel, Z. PROSPE—Programs for ROtational SPEctroscopy. http://info.ifpan.edu.pl/~kisiel/prospe.htm (accessed April 22, 2023).
(45) Frisch, M. J.; Trucks, G. W.; Schlegel, H. B.; Scuseria, G. E.; Robb, M. A.; Cheeseman, J. R.; Scalmani, G.; Barone, V.; Petersson, G. A.; Nakatsuji, H.; et al. *Gaussian 16*; Gaussian, Inc.: Wallingford, CT, 2016.
(46) Schmidt, J.; Polik, W. *WebMO Enterprise, 20.0.012e*; WebMO LLC: Holland, MI, 2020. www.webmo.net (accessed Jan 11, 2024).
(47) CFOUR, a quantum chemical program package written by Stanton, J. F.; Gauss, J.; Cheng, L.; Harding, M. E.; Matthews, D. A.; Szalay, P. G. with contributions from Auer, A. A.; Bartlett, R. J.; Benedikt, U.; Berger, C.; et al. For the current version, see http://www.cfour.de (accessed Jan 14, 2024).
(48) Mills, I. M. Vibration-Rotation Structure in Asymmetric- and Symmetric-Top Molecules. In *Molecular Spectroscopy: Modern Research*; Rao, K. N., Mathews, C. W., Eds.; Academic Press: New York, 1972; Vol. *1*, pp 115−140.
(49) Schneider, W.; Thiel, W. Anharmonic Force Fields from Analytic Second Derivatives: Method and Application to Methyl Bromide. *Chem. Phys. Lett.* **1989**, *157*, 367−373.
(50) Stanton, J. F.; Lopreore, C. L.; Gauss, J. The Equilibrium Structure and Fundamental Vibrational Frequencies of Dioxirane. *J. Chem. Phys.* **1998**, *108*, 7190−7196.
(51) Esselman, B. J.; Pimentel, E. B.; Styers, W. H.; Jean, D. R.; Woods, R. C.; McMahon, R. J. The 235−360 GHz Rotational Spectrum of 1-Oxaspiro[2.5]octa-4,7-dien-6-one—Analysis of the Ground Vibrational State and Its 10 Lowest-Energy Vibrationally Excited States. *J. Phys. Chem. A* **2024**, *128*, 191−203.
(52) Dorman, P. M.; Esselman, B. J.; Changala, P. B.; McCarthy, M. C.; Woods, R. C.; McMahon, R. J. Rotational spectra of twenty-one vibrational states of [^{35}Cl]-and [^{37}Cl]-chlorobenzene. *J. Mol. Spectrosc.* **2023**, *394*, 111776.
(53) Esselman, B. J.; Zdanovskaia, M. A.; Woods, R. C.; McMahon, R. J. Millimeter-wave Spectroscopy of the Chlorine Isotopologues of 2-Chloropyridine and Twenty-Three of Their Vibrationally Excited States. *J. Mol. Spectrosc.* **2019**, *365*, 111206.
(54) Higgins, P. M.; Esselman, B. J.; Zdanovskaia, M. A.; Woods, R. C.; McMahon, R. J. Millimeter-wave Spectroscopy of the Chlorine Isotopologues of Chloropyrazine and Twenty-Two of Their Vibrationally Excited States. *J. Mol. Spectrosc.* **2019**, *364*, 111179.

(55) Orr, V. L.; Esselman, B. J.; Dorman, P. M.; Amberger, B. K.; Guzei, I. A.; Woods, R. C.; McMahon, R. J. Millimeter-wave Spectroscopy, X-ray Crystal Structure, and Quantum Chemical Studies of Diketene - Resolving Ambiguities Concerning the Structure of the Ketene Dimer. *J. Phys. Chem. A* **2016**, *120*, 7753−7763.
(56) Walters, N. A.; Amberger, B. K.; Esselman, B. J.; Woods, R. C.; McMahon, R. J. Millimeter-wave Spectroscopy of *syn* Formyl Azide ($HC(O)N_3$) in Seven Vibrational States. *J. Mol. Spectrosc.* **2017**, *331*, 71−81.
(57) Gordy, W.; Cook, R. L. Microwave molecular spectra, 3rd ed.; Wiley New York: New York, 1984. http://catalog.hathitrust.org/api/volumes/oclc/11090587.html.
(58) Motiyenko, R. A.; Margulès, L.; Alekseev, E. A.; Guillemin, J. C.; Demaison, J. Centrifugal distortion analysis of the rotational spectrum of aziridine: Comparison of different Hamiltonians. *J. Mol. Spectrosc.* **2010**, *264*, 94−99.
(59) Margulès, L.; Perrin, A.; Demaison, J.; Merke, I.; Willner, H.; Rotger, M.; Boudon, V. Breakdown of the reduction of the rovibrational Hamiltonian: The case of $S^{18}O_2F_2$. *J. Mol. Spectrosc.* **2009**, *256*, 232−237.
(60) Watson, J. K. G. Determination of Centrifugal Distortion Coefficients of Asymmetric Top Molecules. *J. Chem. Phys.* **1967**, *46*, 1935−1949.
(61) Winnewisser, G. Millimeter Wave Rotational Spectrum of HSSH and DSSD. II. Anomalous *K* Doubling Caused by Centrifugal Distortion in DSSD. *J. Chem. Phys.* **1972**, *56*, 2944−2954.
(62) Typke, V. Centrifugal distortion analysis including P^6-terms. *J. Mol. Spectrosc.* **1976**, *63*, 170−179.
(63) van Eijck, B. P. Reformulation of quartic centrifugal distortion Hamiltonian. *J. Mol. Spectrosc.* **1974**, *53*, 246−249.
(64) Bunn, H. A.; Esselman, B. J.; Franke, P. R.; Kougias, S. M.; McMahon, R. J.; Stanton, J. F.; Widicus Weaver, S. L.; Woods, R. C. Millimeter/Submillimeter-wave Spectroscopy and the Semi-experimental Equilibrium (r_e^{SE}) Structure of 1*H*-1,2,4-Triazole (c-$C_2H_3N_3$). *J. Phys. Chem. A* **2022**, *126*, 8196−8210.
(65) McKean, D. C.; Craig, N. C.; Law, M. M. Scaled Quantum Chemical Force Fields for 1,1-Difluorocyclopropane and the Influence of Vibrational Anharmonicity. *J. Phys. Chem. A* **2008**, *112*, 6760−6771.
(66) Zdanovskaia, M. A.; Franke, P. R.; Esselman, B. J.; Billinghurst, B. E.; Zhao, J.; Stanton, J. F.; Woods, R. C.; McMahon, R. J. Vibrationally excited states of 1*H*- and 2*H*-1,2,3-triazole isotopologues analyzed by millimeter-wave and high-resolution infrared spectroscopy with approximate state-specific quartic distortion constants. *J. Chem. Phys.* **2023**, *158*, 044301.
(67) Aliev, M. R. Vibrational dependence of the quartic centrifugal constant and the octic centrifugual constant of linear molecules. *Opt. Spectrosc.* **1986**, *60*, 411−412.
(68) Demaison, J.; Margulès, L.; Boggs, J. E. Equilibrium structure and force field of NH_2. *Phys. Chem. Chem. Phys.* **2003**, *5*, 3359−3363.
(69) Margulès, L.; Motiyenko, R. A.; Demaison, J. Millimeterwave and submillimeterwave spectra of sulfur dioxide $^{32}S^{16}O^{18}O$ and $^{32}S^{18}O_2$, centrifugal distortion analysis and equilibrium structure. *J. Quant. Spectrosc. Radiat. Transfer* **2020**, *253*, 107153.
(70) Tyuterev, V.; Tashkun, S.; Rey, M.; Nikitin, A. High-order contact transformations of molecular Hamiltonians: general approach, fast computational algorithm and convergence of ro-vibrational polyad models. *Mol. Phys.* **2022**, *120*, No. e2096140.
(71) Tyuterev, V.; Tashkun, S.; Seghir, H. High-order contact transformations: general algorithm, computer implementation, and triatomic tests. *Proc. SPIE* **2004**, *5311*, 164−175.
(72) Watson, J. K. G. Higher-order vibration-rotation energies of the X_3 molecule. *J. Mol. Spectrosc.* **1984**, *103*, 350−363.

https://doi.org/10.1021/acs.jpca.3c08002
J. Phys. Chem. A 2024, 128, 1427−1437